THE EFFECT OF AN OUTER-ELEMENT BOW ON DRYOUT POWER AND POST-DRYOUT HEAT TRANSFER OF A 37-ELEMENT BUNDLE STRING

S.C. Sutradhar

Fuel Channel Thermalhydraulics Branch
Chalk River Laboratories
Chalk River, Ontario K0J 1J0
Canada

ABSTRACT

Dryout and post-dryout tests were performed with a modified 37-element simulated CANDU® fuel string, with one outer element of the last bundle gradually bowed toward the flow-tube wall. The element had 8% higher heat flux than the remaining outer-ring elements and had the narrowest gap between it and the flow-tube wall. The initial dryout occurred on the bowed element for all element-to-wall gap sizes. The dryout power decreased moderately (4% average) as the gap size was reduced to 13.5% of the nominal (unbowed) gap. For smaller than 13.5% gaps, however, the dryout power increased slightly (1.2%) at the low (10.5 kg/s) flow rate and decreased by 5% at the high (16.0 kg/s) flow rate, compared to the nominal gap dryout power. Surface temperatures of the bowed element were recorded for different gap sizes and up to 20% overpower (maximum). The temperature increased by 26% at the maximum overpower as the element was moved from nominal to zero gap position.

INTRODUCTION

An element within a fuel bundle may distort because of a number of mechanisms, either within the fuel element or external to it. One mode of distortion is element bowing, either toward an adjacent element or toward the pressure tube. Bowing may occur because of the differential thermal expansion caused by large circumferential temperature gradients on an element. These gradients could result from improper coolant circulation and neutron flux variation in a fuel bundle.

During a postulated loss-of-coolant accident (LOCA) in a CANDU reactor, non-uniform fuel heat-up at or near nominal element power over an extended period of time may lead to the distortion of a fuel element. A severely distorted element may cause (i) localized pressure-tube overheating, (ii) sheath failure or (iii) permanent element deformation or both (ii) and (iii).

As an element distorts, coolant circulation around it changes significantly. The heat-transfer coefficient deteriorates locally, leading to an escalation in the circumferential temperature gradient on that element. If the element encounters a severe temperature gradient during the post-dryout (PDO) situation, it may deform permanently. The permanently deformed element could potentially affect the dryout power or critical heat flux (CHF) of the bundle during

---

CANDU®: CANada Deuterium Uranium, a registered trademark of AECL.

subsequent reactor operation. However, for bowed elements closer to the flow-tube wall, the cold wall effect would dominate and this could lead to improved cooling for those elements (Kunsemiller 1965, and Sutradhar and Schenk 1997).

To gain knowledge of dryout behaviour and variation in surface temperature around a severely distorted element, several tests were performed at the Chalk River Laboratories (CRL) starting with annular test sections (Huang et al. 1996). Because these tests in simple geometries do not represent the complex flow phenomena in real bundles, dryout and PDO tests in a full-scale, simulated 37-element CANDU fuel string were performed at CRL in 1995. One outer element of the downstream-most bundle was bowed at gradual (but controlled) steps toward the flow-tube wall. Both dryout power and PDO surface-temperature data were obtained using Freon-134a refrigerant as the coolant. Sutradhar and Schenk (1997) presented the results of the effect of element bow on dryout power and PDO heat transfer. The bowed element in their study had no bearing pads. As a first attempt to study the element bow in a full-scale bundle, a simplistic approach (without bearing pads on the bowed element) was taken. Later it was realised that the absence of bearing pads might have adversely affected (because of reduced turbulence) the dryout and PDO behaviour of the bowed element, and hence, of the bundle string.

Subsequently, the bowed element of the fuel string was modified to include simulated bearing pads, and further tests were performed in 1997. This paper presents the results of the 1997 test for dryout power and the surface-temperature distributions (at PDO conditions) of the bowed element. The objectives of the test are to investigate the effect of outer element bow on dryout power and to generate surface-temperature profiles for the bowed element at PDO conditions. The results may be used to validate relevant prediction techniques applicable to CANDU fuel bundles with distorted or bowed outer fuel elements.

EXPERIMENTAL APPARATUS AND PROCEDURE

Loop Facility

The MR-3 Freon heat-transfer loop at CRL allows heat-transfer tests to be performed on a string of 12 full-scale CANDU fuel bundles. Freon-134a (DuPont tradename for tetra-fluoroethane) cools the test section at a much lower pressure, temperature and power, thus reducing cost and time relative to water tests. Liquid refrigerant circulates, at a measured and controlled rate, temperature and pressure through the vertical test section. The test section is heated by a continuously adjustable dc power supply (maximum 1 700 kW).

Test Section

The test section was a 37-element, 12-bundle CANDU fuel string, including end plates, bearing pads and inter-element spacers. One outer element (# 8 in Figure 1) of the downstream-most bundle was modified for the test. The element had 8% higher heat flux, over 1.5-m length, than the other elements in the outer ring; this modification ensured initial dryout to occur on the intended element. The element was slightly prebowed (0.2 mm), and the maximum bow was located 80 mm from the downstream end of the bundle (Figure 2). The location was also the point of closest approach to the flow-tube wall. A 0.2-mm thick metal strip, welded at the downstream end of the element, compensated for the prebow. As the bowed element was moved toward the flow tube, the metal strip and the point of maximum bow contacted the tube at the same time. The metal strip was used to activate an electrical circuit (Figure 3) once the element contacted the flow tube. As the element moved toward the flow tube the space between them reduced progressively. Hence, simulated (leaf-spring type) bearing pads were welded on the bowed element: one at the mid-plane and the other at the upstream end of the element. With regular bearing pads, the element could not have been moved toward the flow tube, and no simulation for the zero gap would have been possible. The bundle string, otherwise, had a uniform axial heat-flux distribution, and a natural-uranium (NU) radial heat-flux profile.

The desired gap size between the bowed element and the flow-tube wall was maintained by moving the element in the radial direction, using a cam-drive mechanism. The mechanism was mounted downstream of the bundle string to circumvent any interference with the thermalhydraulic phenomena around the dryout location on the bowed element. The accurately calibrated smooth cam was positioned on the central element and downstream of the last end plate. A solid rod through the copper extension tube above the central element connected the cam to an electric motor, and the motor was positioned outside the test section.

A transverse push rod, between the copper extension rods of elements 23 and 24 (Figure 3), glided smoothly over the cam. As the cam was rotated, the push rod moved the bowed element in and out, depending on the direction of cam rotation. Once the element touched the tube wall, an electrically activated small brass insert, mounted flush with the tube wall, indicated its contact with the wall. At this point, further travel of the bowed element was halted.

Before inserting the bundle string into the flow tube, the radial movement of the bowed element was calibrated against the angular rotation of the cam. The bundle string was then inserted fully inside the flow tube and the bowed element was slowly brought in contact with the tube wall. The contact signal went off when the metal strip on the element touched the brass insert in the flow tube. The nominal gap between the bowed element and the flow-tube wall, corresponding to the angular rotation of the cam, was read from the calibration chart. The nominal gap was also equal to the maximum travel of the bowed element. The bundle string was mounted eccentrically so that the bearing pads on elements 7, 8, and 9 were in contact with the flow-tube wall.

Sliding thermocouples in the bowed element and in 4 surrounding elements (7, 9, 23, and 24 in Figure 1) of the last bundle recorded their surface temperatures. Axial travel of thermocouples in each element was from 16.0 mm, measured from the end of the bundle, up to about half-bundle length, and their angular rotation was 360^{o}. Each slider had 2 thermocouples (in case 1 failed during testing). The zero-degree line on each element was radially outward and closest to the tube wall. The thermocouples were rotated clockwise (during PDO tests), looking upstream along individual elements.

Test Procedure

Seven element-to-wall gap sizes, including the nominal (1.0 mm or 100% gap) and zero gaps, were tested for dryout power at 1.65 MPa pressure, 10 to 16 kg/s flow rate, and 40 to 54^{o}C inlet temperature (water equivalent conditions are 9.6 MPa pressure, 15 to 22 kg/s flow rates, and 260 to 300^{o} inlet temperatures). The PDO tests were performed at four overpowers, 10.5 kg/s flow rate, 54^{o}C inlet temperature and for different gap sizes. (Tests were performed only at one pressure to investigate the effect of element bow on dryout power, and if the effect had been severe, then tests at other pressures would have been performed.)

<u>Initial dryout power:</u> For the nominal gap size and a selected test condition, the test-section power was increased in small steps to the anticipated dryout power. The bowed element and 4 of its neighbouring elements were scanned thoroughly for the initial dryout at each power increment. The initial dryout power was recorded when the element-surface temperature jumped by 3 to 5^{o}C. Then the test-section power was reduced slightly (2 to 5 kW). Any variations in the loop conditions from the set ones were re-set, and the power was raised slowly to confirm the initial dryout. The on-line data acquisition system recorded the pre-assigned test parameters. Then the power was reduced to rewet the element; the gap size was changed, and the procedure was repeated for other test conditions and gap sizes.

<u>PDO temperature profile:</u> The element-surface temperatures at PDO conditions were measured for different gap sizes. For each gap size, the initial dryout power of the bundle was measured first. Then the thermocouples were positioned at the downstream location and aligned to the 0^{o} lines (facing the flow-tube wall) in bowed element and 4 surrounding elements. They were traversed (by robotics) axially down at 10-mm steps along the 0^{o} lines. They were allowed to travel slightly past the upstream drypatch boundary on the bowed element. Next the thermocouples were rotated 20^{o} clockwise, and were moved axially up at 10-mm steps. Once the scanning for the entire surface of the elements was completed, the power was increased to the next (10%) overpower value; the scanning process was repeated. The power was reduced and the next gap size was chosen; the process was repeated to cover the planned gap sizes and overpowers.

RESULTS AND DISCUSSIONS

<u>Initial Dryout for Nominal Gap Size</u>: For the nominal gap size between bowed element and the flow-tube wall, the initial dryout always occurred on, and close to the end of, the bowed element. The dryout occurred because (i) the bowed element had about 8% higher heat flux than the remaining outer-ring elements, (ii) the 1.0-mm gap was the smallest in the bundle, and (iii) the bowed element had 2 leaf springs (without these bearing pads, the dryout occurred slightly upstream of the end of the heated length, Sutradhar and Schenk 1997). The angular spread of the location of the nominal gap dryout was approximately ±5^{o} from the 0^{o} line. Figure 4 depicts, as expected, a linear variation of nominal gap dryout power with inlet temperature.

<u>Initial Dryout for Changing Gap Sizes:</u> In all cases, the initial dryout power decreased as the gap size was gradually reduced from the nominal to about the 13.5% gap size; the decrease was 4% (average of all the runs) from that for the nominal gap size. The dryout power increased, albeit

marginally, for gap sizes smaller than 13.5%. The increase may be attributed to the cold wall effect of the flow tube. The dryout power for the zero gap size (bowed element contacting the wall), on average, was 2.4% higher than that for the 13.5% gap size, but was 1.6% lower than that for the nominal gap size. The range of change in dryout power for zero gap (compared to the nominal gap) was from -5% (at 16.0 kg/s) to 1.2% (at 10.5 kg/s). The variations in dryout power with changing gap size are shown in Figures 5 to 7, respectively, for 40^{o}C, 47^{o}C, and 54^{o}C inlet temperatures, and 1.65 MPa pressure. The results for 3 mass-flow rates are plotted in each figure.

As the gap size progressively narrowed from the nominal gap size (to about 13.5%), the dryout location (on the bowed element) remained on the narrow strip (±5^{o}), facing the flow-tube wall. At about the 13.5% gap size, an angular shift in the dryout location was noticed. A further reduction in the gap size (from 13.5%) also caused the dryout location to travel upstream; the maximum travel was 45 mm and the angular spread was from +5^{o} to -15^{o}. In most cases, the initial dryout locations for gap sizes smaller than 13.5% were in the outer subchannel between element 8 and element 7. The maximum uncertainty in the measured dryout power was ±1.2%.

PDO Temperature Profiles for Changing Gap Sizes

The PDO temperature profiles of elements 7, 8, 9, 23, and 24 were obtained at 4 overpowers and for different element-to-wall gap sizes. However, only the results of element 8 are presented here.

$$Overpower(\%) = \frac{Power - Dryout\ Power\ \ for\, a\, Gap}{Dryout\ Power\ \ for\, a\, Gap} X100$$

The overpowers used in the present test were 0%, 10%, 15%, and 20%, and the results for 100% (nominal), 47% and 0% (contact) gap sizes are discussed.

The temperature profiles on element 8 were slightly asymmetric about the 0^{o} line, because the bowed element was closer to element 7 than to element 9 (due to manufacturing tolerances). Hence, the maximum temperature of the bowed element was recorded mostly between 320^{o} to 360^{o} angular location.

Temperature profiles for the nominal gap size: Figure 8 shows no perceptible drypatch on element 8 at 0% overpower (i.e., at initial dryout power). But at 10% overpower, the downstream end of the element was in wraparound dryout. The maximum temperature (about 80^{o}C) was at 30 mm axial and 355^{o} circumferential location, i.e., slightly toward the outer subchannel formed by the flow tube, and elements 7 and 8.

Figure 8 also shows that the drypatch area increased further (up to 150 mm along the 90^{o} line) at 15% overpower. The maximum temperature was about 85^{o}C and occurred at 350^{o} circumferential location. The downstream end, from 0 to 45 mm was in wraparound dryout. The 20% overpower caused a further increase in the drypatch area, and the upstream boundary extended up to 190 mm. The hottest spot (95^{o}C) was at 30 mm axial and 340^{o} circumferential location. The wraparound drypatch enlarged too, extending up to 70 mm from the downstream end of the element.

<u>Temperature profiles for the 47% gap size:</u> Figure 9 shows no drypatch on element 8 at 0% overpower. A drypatch appeared on this element at 10% overpower. The upstream boundary of the drypatch extended up to 105 mm and a part of the surface near the end (up to 20 mm) was in wraparound dryout. The maximum temperature was about 85°C.

The drypatch extended up to 130 mm at 15% overpower. The 20% overpower caused a wraparound dryout on element 8, extending up to 60 mm. The upstream boundary of the drypatch extended up to 180 mm. (The missed upstream drypatch boundary is due to premature stoppage of the downward travel of the thermocouple slider.) The hottest spot (about 95°C) was at 350° and close to the end of the element.

<u>Temperature profiles for the zero gap size:</u> Figure 10 shows dryout on the bowed element near the maximum bow location at 0% overpower. Mild fluctuations in surface temperature were observed in most cases for the zero gap size. The drypatch grew in size at 10% overpower. The upstream boundary of the drypatch extended up to 140 mm, and a wraparound dryout occurred on the downstream end (up to 30 mm). The hottest spot was in the vicinity of the maximum bow location, but slightly toward element 7.

The drypatch on element 8 extended up to 160 mm at 15% overpower. The hottest spot was at 60 mm, facing slightly toward the outer subchannel formed by the flow-tube wall, and elements 7 and 8. As the element touched the wall, the downstream end of the element cooled off slightly. A wraparound dryout, extending up to 65 mm, occurred at this overpower.

The drypatch boundary on element 8 extended up to 210 mm at 20% overpower. The part of the element, from 0 to 75 mm, had a wraparound dryout at this overpower. The hottest spot (120°C, an increase of about 26% from that for the nominal gap) was at the maximum bow location and was slightly toward element 7.

A comparison of the 20% overpower plots in Figures 8 and 10 shows that the drypatch boundaries only changed moderately for the nominal to zero gap sizes. In Figure 8, the wraparound drypatch extended up 60 mm, and in Figure 10 it is up to 75 mm, from the end of the element. The drypatch boundary moved upstream only by 20 mm (190 mm versus 210 mm), as the gap size was reduced from nominal to zero.

CONCLUSIONS

Dryout and post-dryout tests were performed with a modified 37-element simulated fuel string cooled by Freon-134a. One outer element of the last bundle was bowed gradually toward the flow-tube wall. That element, with simulated bearing pads, had 8% higher heat flux than did the remaining outer elements. The element was slightly prebowed, maximum bow was 80 mm upstream of the last end plate. The conclusions are

i) The dryout power of the bundle string decreased moderately with decreasing element-to-wall gap size and reached a minimum for the 13.5% of the nominal gap size. The dryout power for this gap size, on average, was 4% lower than that for the nominal gap size. For gaps smaller than 13.5%, however, dryout power increased slightly. The dryout power for the zero gap size, on average, was 1.6% lower than that measured for the nominal gap size.

ii) The Freon test results indicate that the change in gap size, caused by an outer element bow towards the flow tube, has no significant effect on the dryout power of the modified 37-element bundle string.

iii) The PDO test results indicate that the change in gap size did not significantly affect the drypatch area on the bowed element for up to 20% overpower. At the highest overpower, the maximum surface temperature of the bowed element for the zero gap increased by 26% from that for the nominal gap.

ACKNOWLEDGEMENTS

The author would like to thank W.A. McGillis and J.R. Schenk for construction of the test section; J.A. Whelan and B.J. Addicott for operating the MR-3 loop; R.J. Cowhey and J.W. Martin for instrumentation and data acquisition; and S.T. Yin, L.K.H. Leung and S. Doerffer for comments and suggestions. The author also acknowledges the funding provided by COG and AECL for this work.

REFERENCES

Huang, X.C., Cheng, S.C., Groeneveld, D.C. and Rudzinski, K.F., “Analysis of the conjugation effect during convective flow film boiling conditions in an eccentric annular test section”, Nuclear Engineering and Design, 163, 177-190, 1996.

Kunsemiller, D.F., “Multi-rod Forced Flow Transition and Filmboiling Measurements”, GEAP-5073, 1965.

Sutradhar, S.C. and Schenk, J.R., “The Effect of Element Bow on Dryout Power and PDO Heat Transfer in CANDU Fuel Bundles”, 5th International Conference on CANDU Fuel , Toronto, Ontario, Canada, 1997.

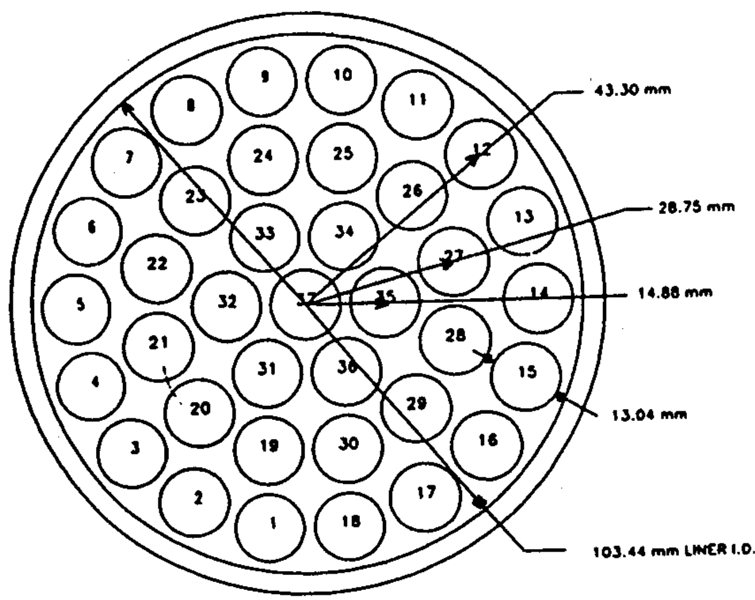

Figure 1: Cross-section of 37-element bundle with element numbering (looking toward the upstream end of the vertical test-section).

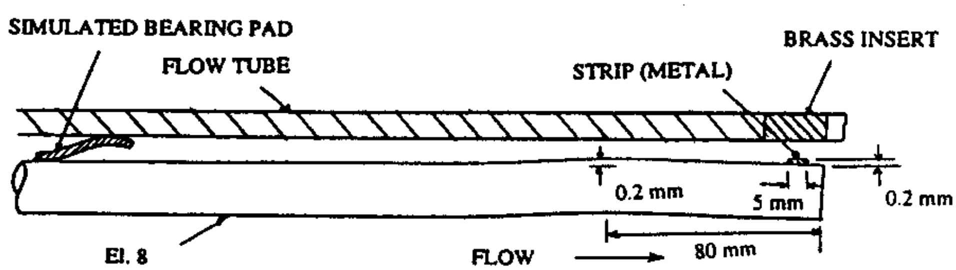

Figure 2: Sketch of the bowed element (#8), showing the thickness of the metal strip and the extent of prebow.

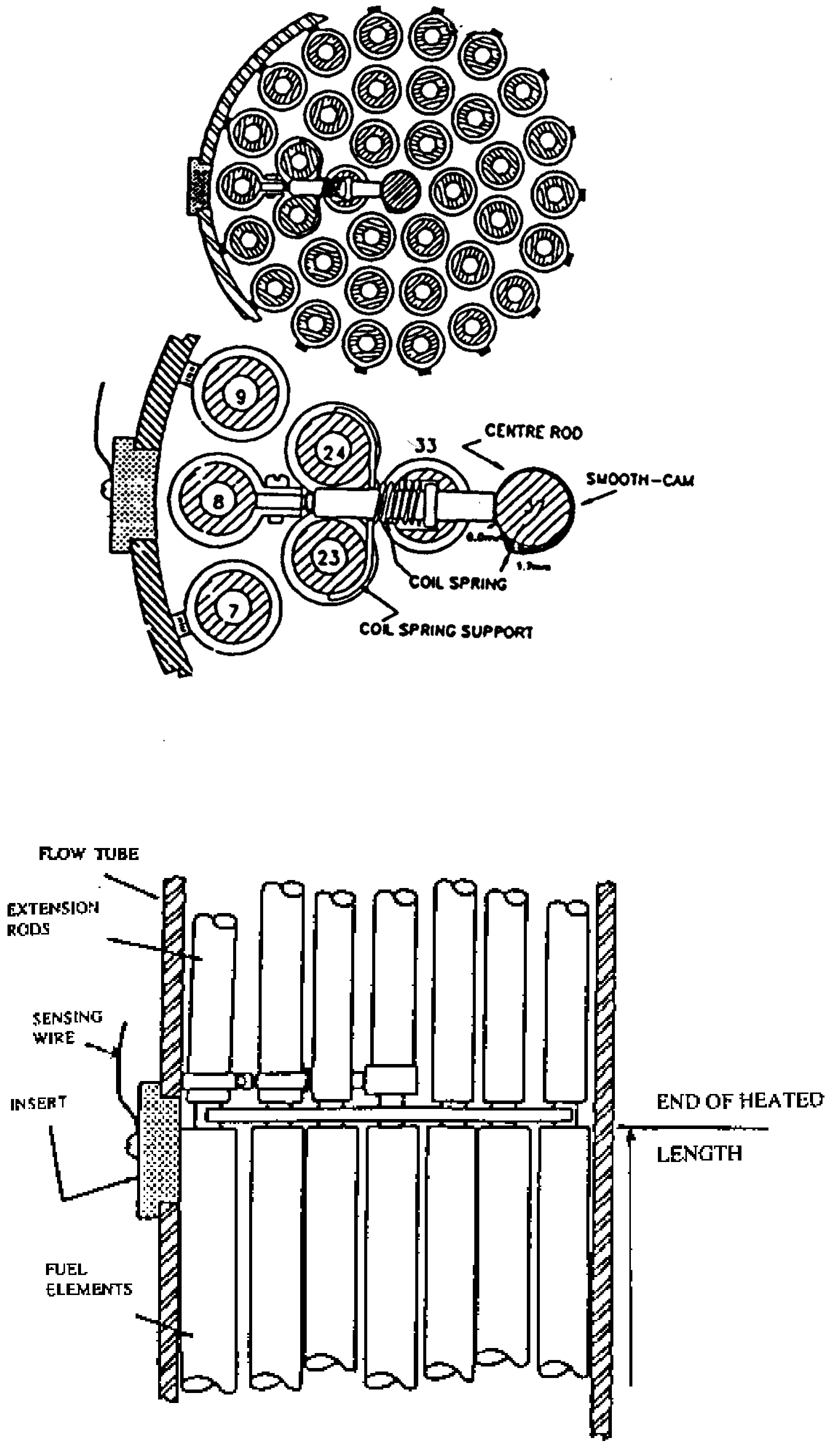

Figure 3: Cam-drive mechanism to move the bowed element in vertical test section (top sketch for nominal gap and bottom sketch for zero gap).

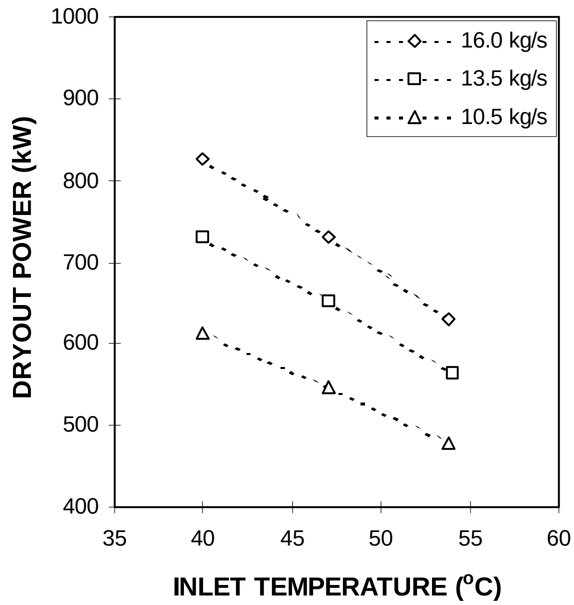

Figure 4: Variation in nominal gap dryout power with coolant inlet temperature.

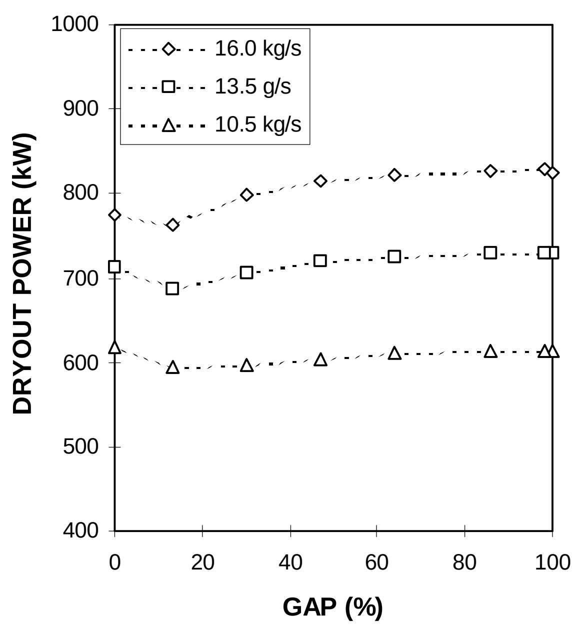

Figure 5: Variation in dryout power with gap size for 40°C inlet temperature.

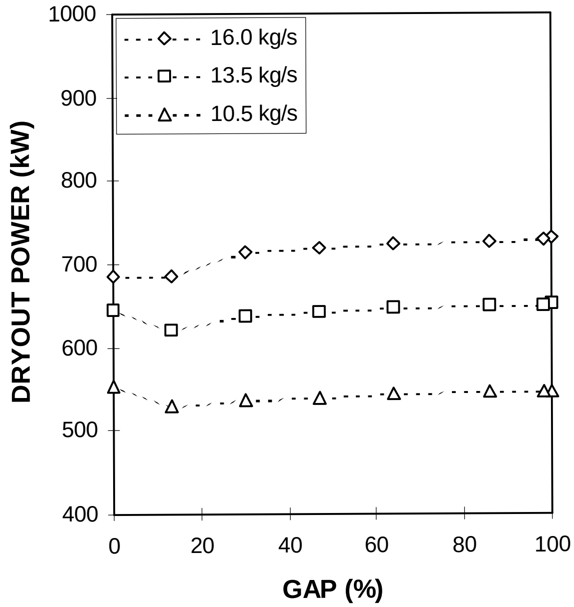

Figure 6: Variation in dryout power with gap size for 47^{o}C inlet temperature.

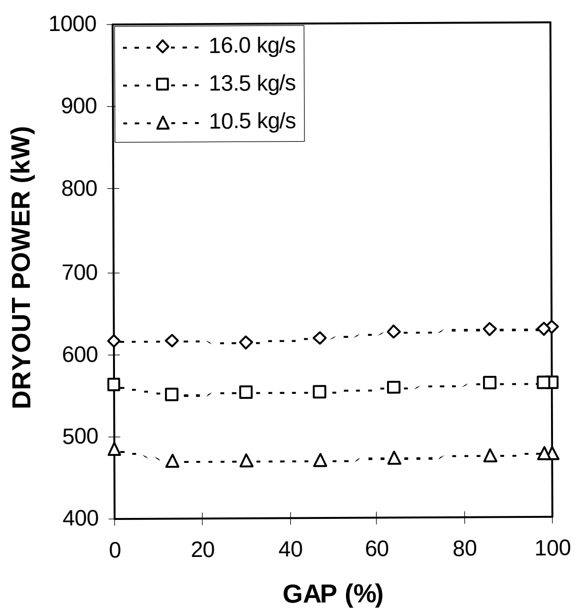

Figure 7: Variation in dryout power with gap size for 54^{o}C inlet temperature.

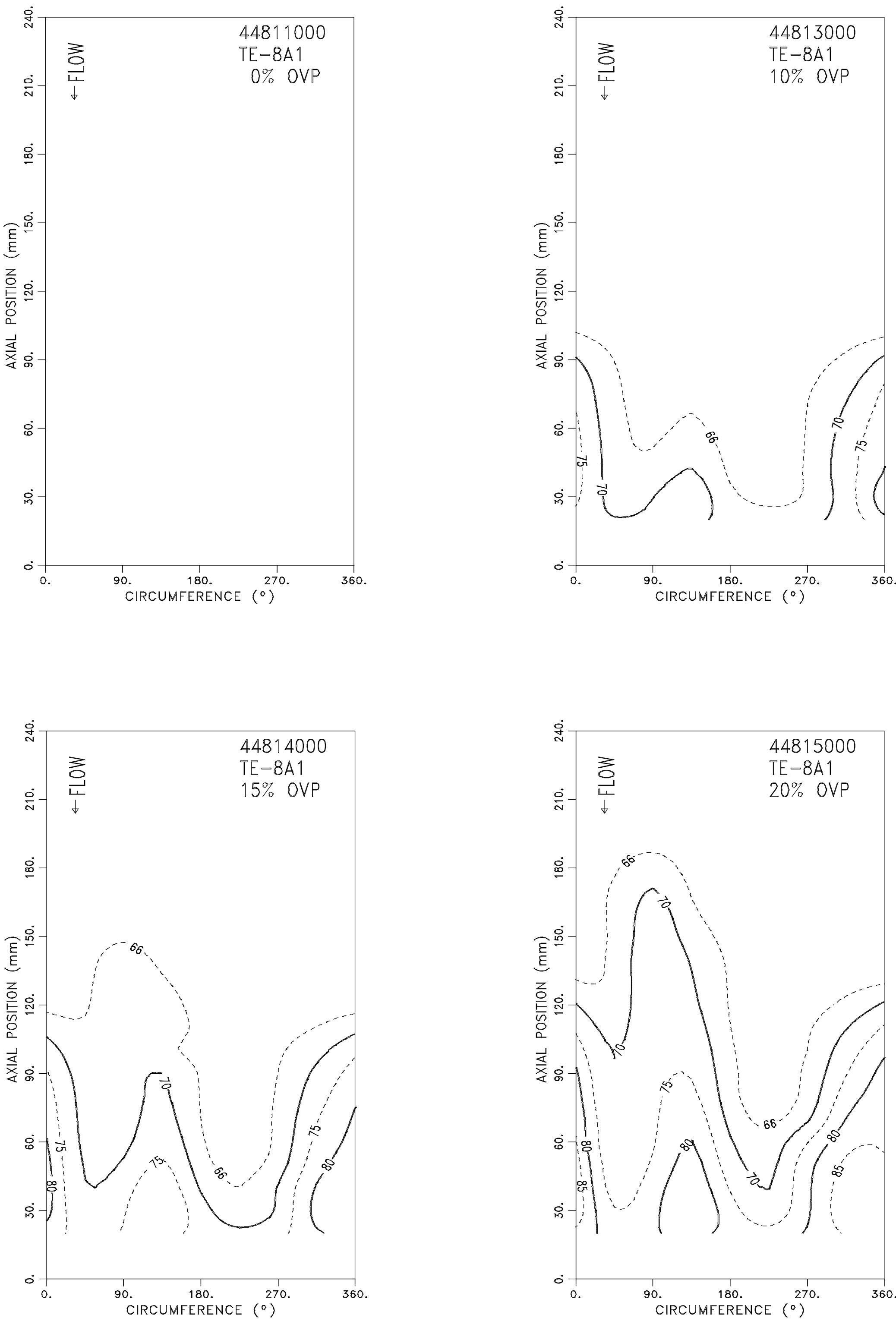

Figure 8: Temperature profiles of bowed element for nominal gap size.

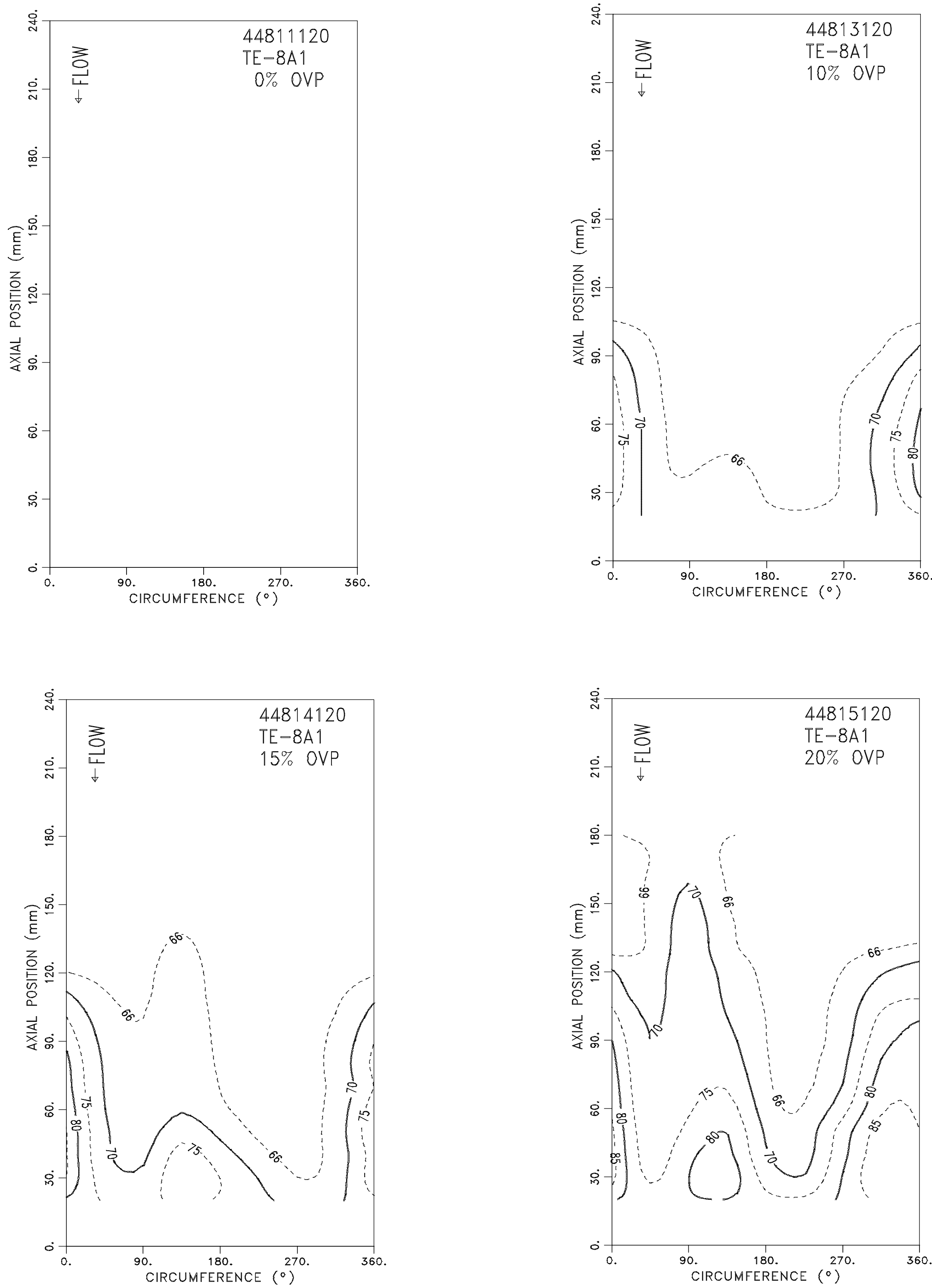

Figure 9: Temperature profiles of bowed element for 47% gap size.

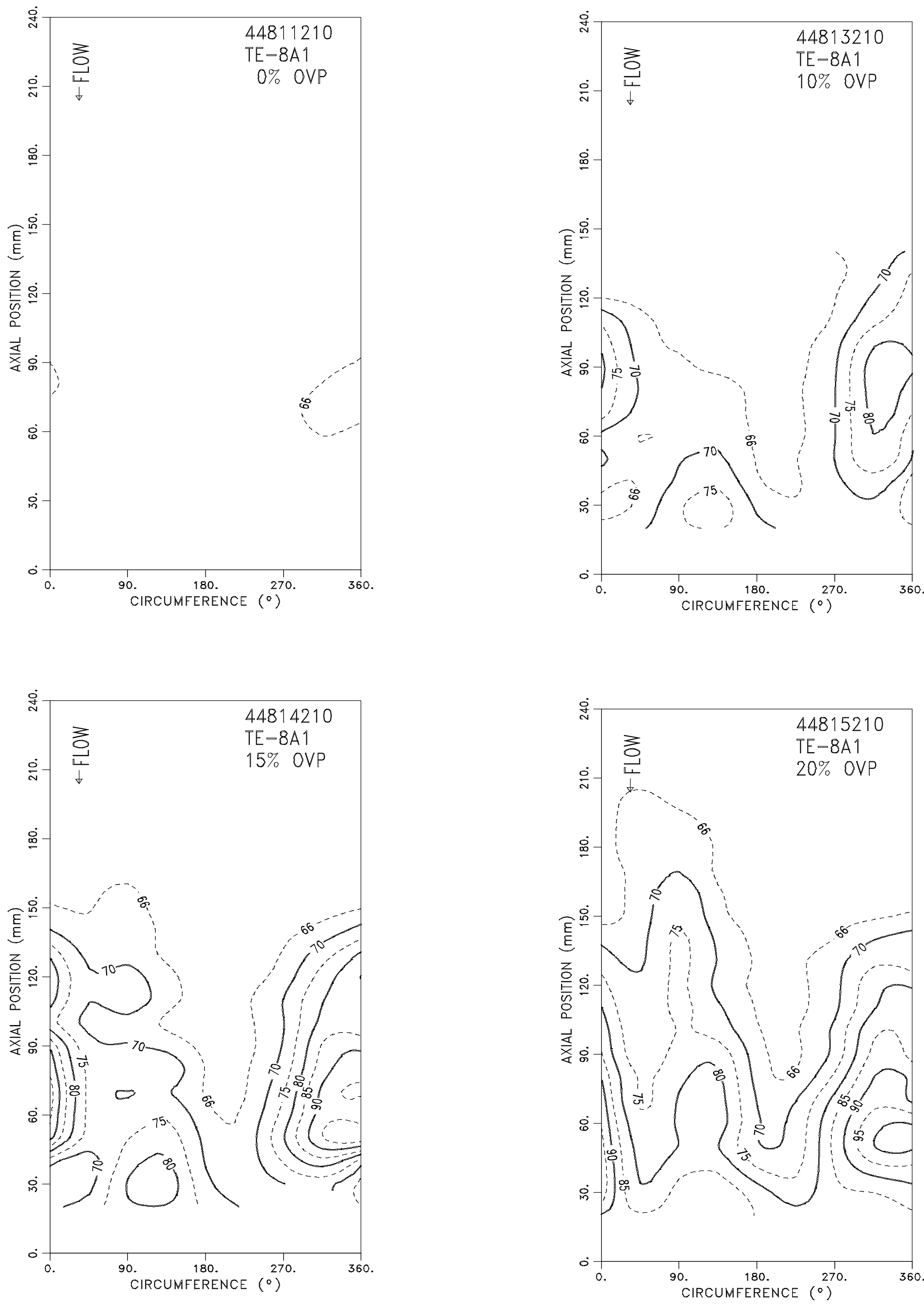

Figure 10: Temperature profiles of bowed element for zero gap size.